LATERAL PHASE SEPARATIONS IN MEMBRANES

E. J. Shimshick, W. Kleemann, W. L. Hubbell,* and H. M. McConnell

Stauffer Laboratory for Physical Chemistry, Stanford, California 94305

Lateral phase separations of phospholipids in both bacterial membranes and model membrane systems (phospholipid bilayers) can be studied using spin labels. Temperature–composition phase diagrams have been determined for binary mixtures of lipids dispersed in excess water by measurements of changes in the fluidity of the membranes as a function of temperature. These results have been used to interpret similar fluidity changes in bacterial membranes. There is evidence that the coexistence of fluid and solid lipid domains facilitates transport through membranes.

Biological membranes have certain properties in common with two-dimensional fluids. Some components of membranes can undergo lateral diffusion in the plane of the membrane. For example, surface antigens have been observed to diffuse laterally in cell hybrids (1, 2) and spin label phospholipids have a high lateral diffusion rate both in model membranes and in biological membranes (3–7). Rapid rotation and translation of rhodopsin in the photorecptor membranes have also been measured (8–10). Pure lipids can undergo phase transitions between a "gel phase," where the hydrocarbon chains are rigid and well-ordered, and a lamellar smectic liquid crystalline phase where the chains are more fluid and less ordered (11–13). These transitions have been observed calorimetrically and spectroscopically in liposomes containing various phospholipids (11, 14, 15). In the membranes of E. coli unsaturated fatty acid auxotrophs, the solidification of the fatty acid chains is detected as changes in the slopes of Arrhenius plots of the transport rate of small molecules across the membrane as a function of temperature. The temperatures at which these changes in slope occur are characteristic of the fatty acids used to supplement the growth medium of the auxotroph (16–19).

Since these membranes contain more than one type of phospholipid, the transitions observed are indicative of phase separations of the lipids into regions of gel phase or S-phase lipids, in our notation, and regions of liquid crystalline phase or F-phase lipids. These phase separations are lateral phase separations. They are two dimensional separations of the lipids, which are initially in one phase and of a specific composition, in the plane of the membrane into regions of S phase of a particular composition and regions of F phase of another composition. This is schematically indicated in Fig. 1. The S and F phases are contiguous and are in equilibrium. A possible illustration of this lateral phase separation is Fig. 2, a freeze-fracture electron micrograph of an equimolar dimyristoylphosphatidylcholine (DMPC)–distearoylphosphatidylcholine (DSPC) dispersion quenched from 35°C, a temperature at which both the fluid and solid phases are present,

*Department of Chemistry, University of California, Berkeley, California 94720

Journal of Supramolecular Structure
© 1973 Alan R. Liss, Inc., 150 Fifth Avenue, New York, N.Y. 10011

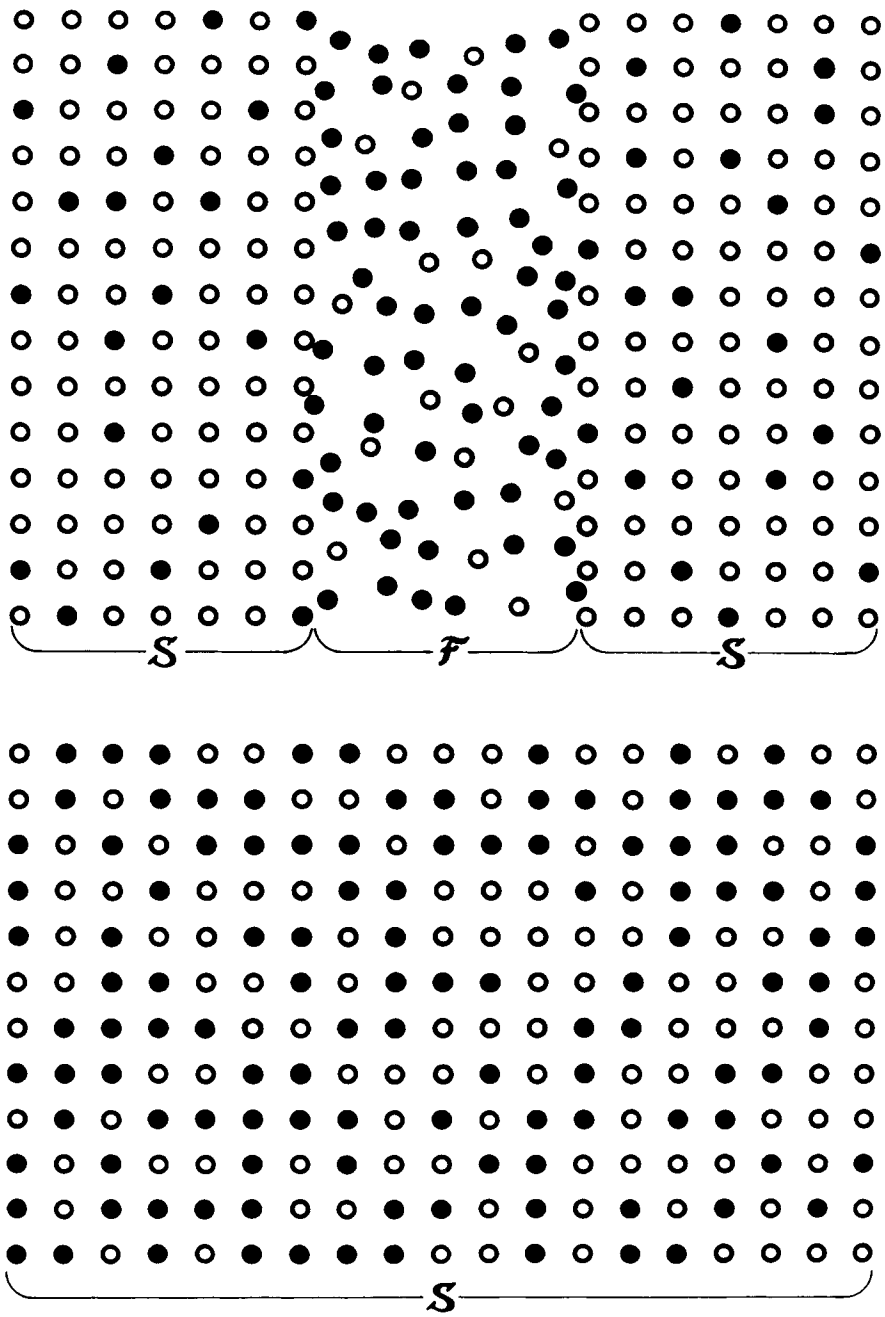

Fig. 1. As shown, a two-dimensional binary mixture which is initially in the S phase laterally separates into F and S phases, each of a different composition, when the temperature is increased.

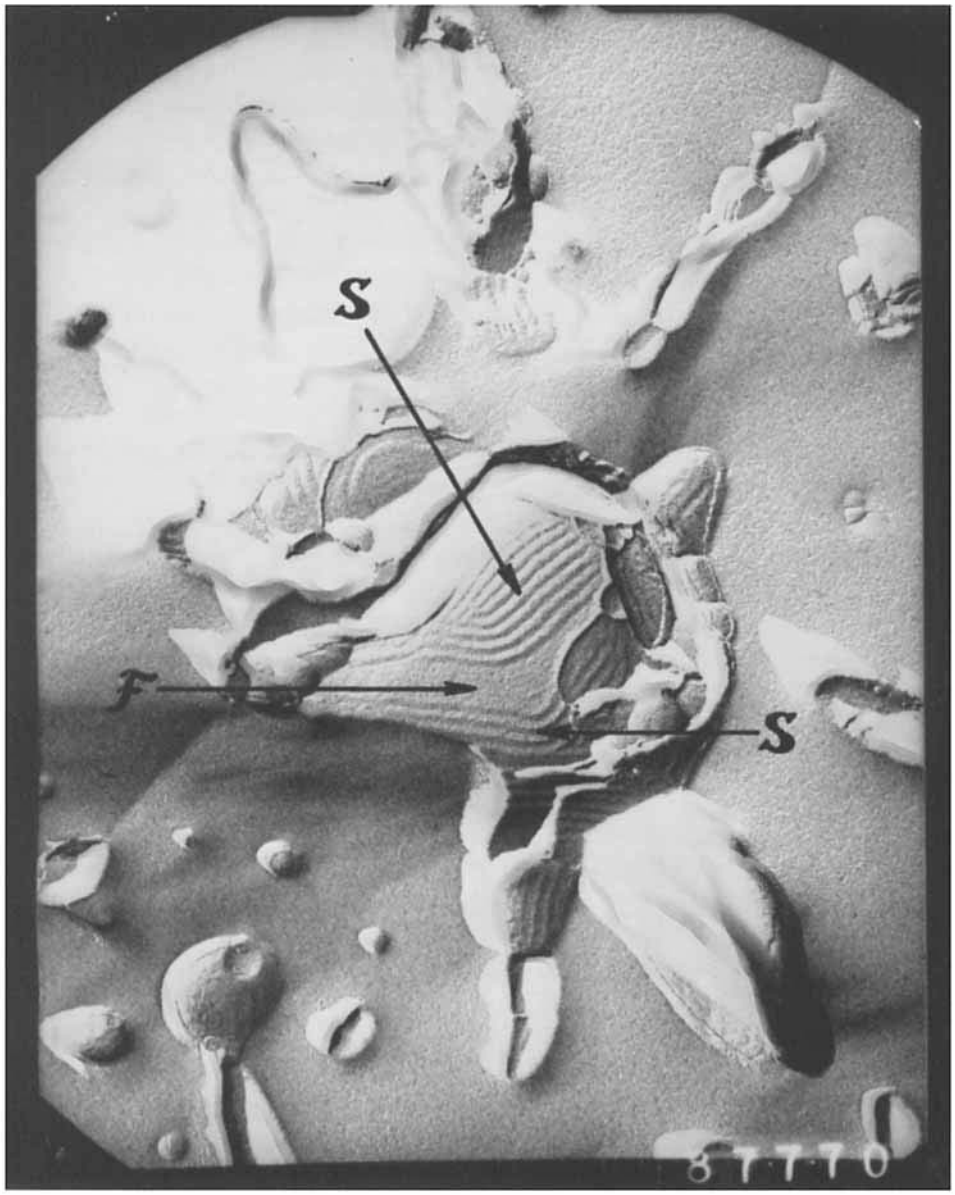

Fig. 2. A freeze-fracture electron micrograph of an equimolar DMPC–DSPC aqueous dispersion quenched from 35°C. The probable identities of the various regions are indicated. The band spacing in the region denoted by S is 192 Å.

as discussed below. Two regions are seen – one composed of quite wide bands which are usually seen when a pure lipid is quenched from below its transition temperature (20), and another composed of quite narrow, indistinct bands. It is likely that these different areas are regions composed of lipids in the S and F phases, respectively. The phase equilibria of these phospholipid systems can be described in terms of a phase diagram, illustrated in Fig. 3, which indicates those temperatures and compositions at which the F

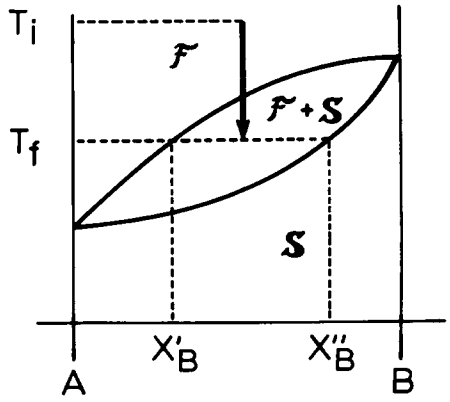

Fig. 3. This temperature-composition plot for two components, A and B, indicates the regions in which the F phase, an equilibrium mixture of F and S phases, and the S phase are present. The upper and lower curves are the fluidus and solidus curves, respectively. If a mixture which is initially in the F phase at a temperature T_i is cooled to a temperature T_f, an equilibrium mixture of F phase with a mole fraction of X' (B) and an S phase with a mole fraction of X'' (B) are formed.

and S phases are stable and those at which an equilibrium mixture of F and S phases is present.

The small spin label, 2, 2, 6, 6-tetramethylpiperidine-1-oxyl, or TEMPO (see illustration), has been used to investigate these phase separations in both bacterial membranes and model membranes (19, 21, 22).

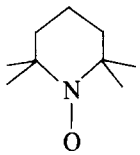

TEMPO partitions between the aqueous phase and the fluid hydrophobic phases present when membranes are dispersed in water (23). The paramagnetic resonance spectrum of TEMPO in an aqueous membrane or phospholipid dispersion is a superposition of two spectra associated with the spin label in the aqueous environment and in the fluid hydrophobic regions of the lipid bilayer. Because of differences in the isotropic g values and hyperfine coupling constants for the spin label in the different environments, the high-field nitroxide hyperfine signal is partially resolved into two components (23). In Fig. 4 the spectrum for TEMPO in an aqueous dispersion of dipalmitoylphosphatidylcholine (DPPC) at 36° is illustrated. The peak amplitude denoted by H is approximately proportional to the amount of spin label dissolved in the fluid hydrophobic regions of the membrane, while that denoted by P is proportional to the amount in the polar, aqueous phase. The relative intensities of these peaks change as the lipid undergoes a phase transition at about 41°C. We measured a TEMPO solubility parameter, f, equal to H/H + P, which is approximately equal to the fraction of the spin label dissolved in the membrane bilayer. In Fig. 4, we also plotted the parameter, f, as a function of temperature for this aqueous DPPC dispersion. The TEMPO solubility decrease abruptly at the calorimetrically measured transition temperature (14). A lesser decrease is observed at a lower temperature corresponding to the so-called "pre-transition" temperature. As the hydrocarbon chains "freeze," TEMPO is excluded from the membrane. We can conclude

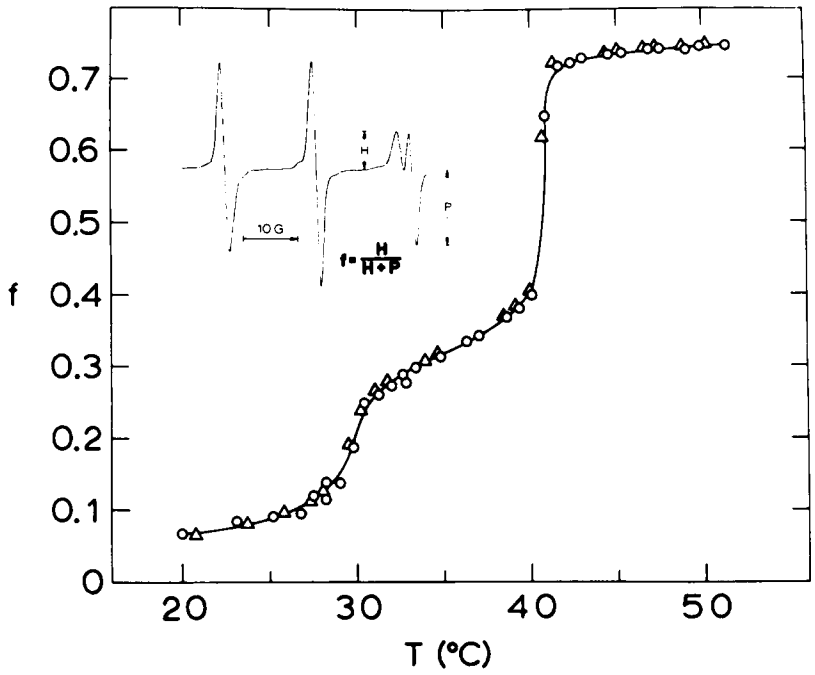

Fig. 4. The TEMPO solubility parameter, f, is plotted as a function of temperature for an aqueous dispersion of DPPC with DPPC/TEMPO mole ratios of 400 and 800.

that the TEMP solubility parameter is a measure of the fraction of the lipids that are in a fluid state or are in the F phase.

For a binary mixture of phospholipids dispersed in excess water, we would expect that the TEMPO parameter vs. temperature curve should exhibit abrupt changes in slope at temperatures corresponding to the onset and completion of phase separation. These high- and low-temperature changes in slope then would give points on the fluidus and solidus curves of an equilibrium phase diagram for the particular composition of phospholipids examined. Phase diagrams for aqueous dispersions of DMPC–DSPC (21) and DMPC–cholesterol (22) are illustrated in Figs. 5 and 6, respectively. TEMPO solubility curves for DMPC–DSPC are illustrated in Fig. 7A for several different mole fractions of of DSPC (21). Straight lines were drawn through each portion of these curves, and the high- and low-temperature changes in slope were used to define points on the phase diagram. For some of these DMPC–DSPC mixtures, the TEMPO parameter–temperature plot shows more than two abrupt changes in slope. However, only the high- and low-temperature changes in slope define the fluidus and solidus curves. We calculated the TEMPO parameter as a function of temperature from the shape of the phase diagram as a check of self-consistency. This calculation used the definition of the TEMPO parameter, the partition coefficient for the spin label between the lipid phase and the aqueous phase, and an equation derived by material balance relating the shapes of the fluidus and solidus curves and the initial composition of the lipid mixture to the mole fraction of the lipids in the F phase. The calculated curves are illustrated in Fig. 7B for DMPC–DSPC (21). The agreement between the experimental and calculated curves is quite good in light of the approximations used, and we can conclude that we are measuring the

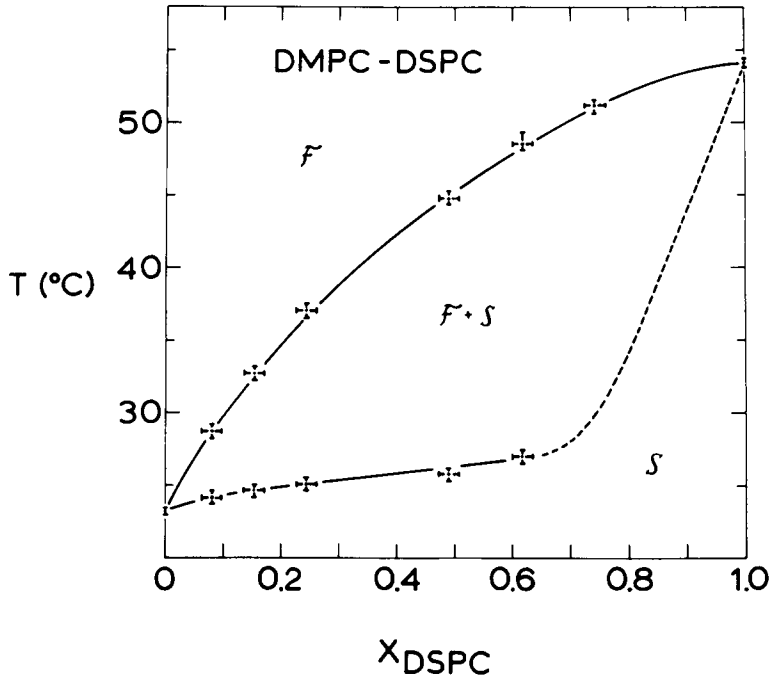

Fig. 5. The phase diagram (temperature vs. mole fraction of DSPC) for aqueous dispersions of the DMPC–DSPC system.

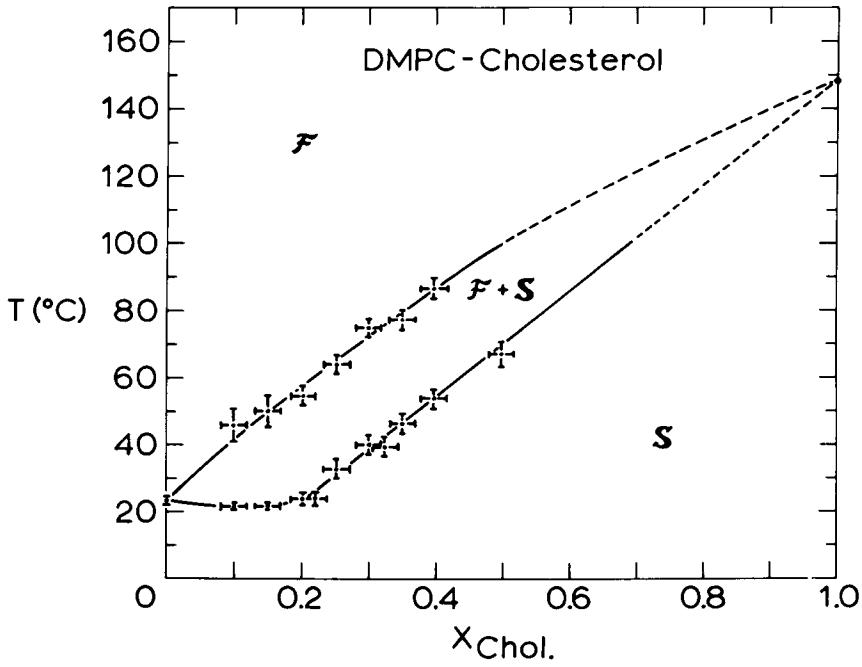

Fig. 6. The phase diagram for the DMPC–cholesterol system. The solidus curve can be extrapolated linearly to the melting point of cholesterol.

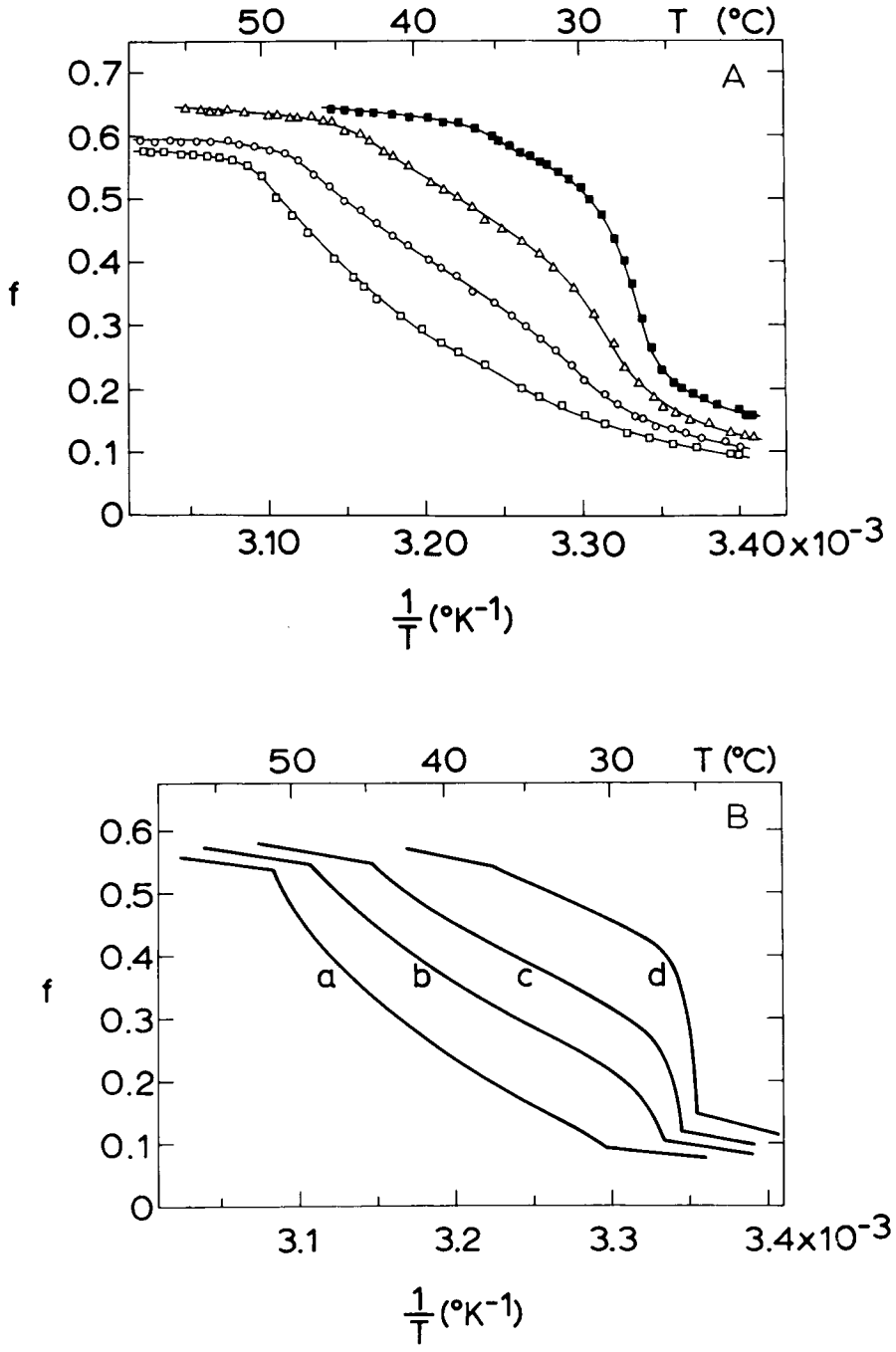

Fig. 7. (A) Experimental TEMPO solubility parameter, f, as a function of 1/T for the DMPC–DSPC system: □ 74 mole % DSPC, ○ 62 mole %, △ 49 mole %, and ■ 24 mole %. (B) Calculated TEMPO solubility parameter, f, as a function of 1/T for: (a) 75 mole % DSPC; (b) 63 mole %; (c) 50 mole %; and (d) 25 mole %.

equilibrium phase diagram of these lipid mixtures. The phase diagrams for DMPC–DSPC, DMPC–cholesterol and for others not shown, such as DPPC–cholesterol, DMPC–dipalmitoylphosphatidyl ethanolamine (DPPE), and DPPC–DPPE, are triangular in shape and indicate some solid immiscibility (21, 22). The phase diagrams for DMPC–DPPC and DPPC–DSPC, on the other hand, are similar to that in Fig. 3 where the two components form a continuous range of solid solutions (21).

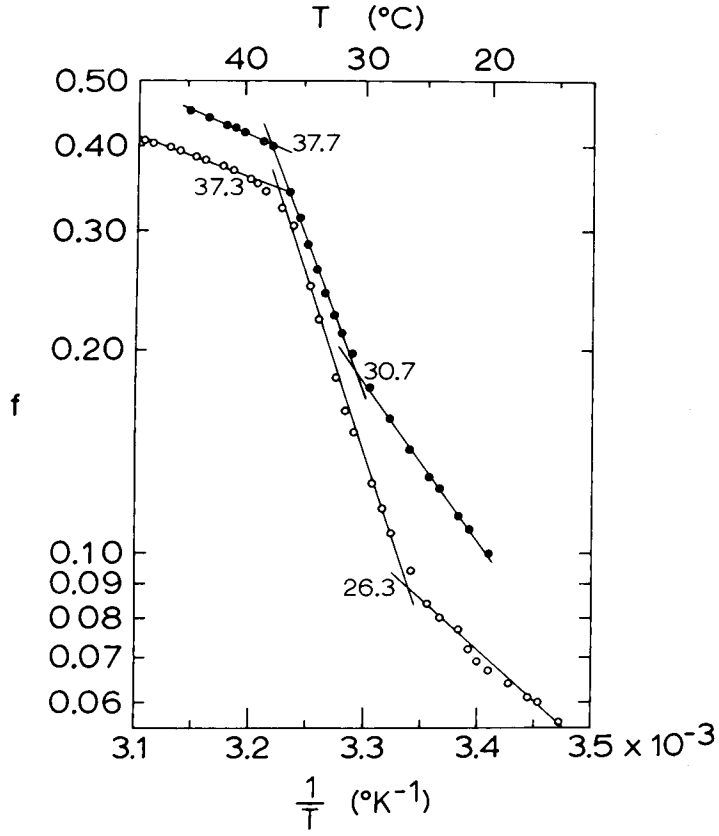

Fig. 8. TEMPO parameter, f, as a function of 1/T for: ● the inner membranes of E. Coli unsaturated fatty acid auxotrophs whose growth medium was supplemented with elaidic acid; and ○ the extracted lipids of these membranes. These membranes and the extracted lipids were obtained from C. Linden and C. F. Fox (19).

The TEMPO solubility curves for both the inner membranes of E. coli fatty acid auxotrophs whose growth medium was supplemented with elaidic acid and the lipids extracted from these membranes are illustrated in Fig. 8 (19). Abrupt changes in slope of the f vs. 1/T curves are observed at temperature close to those at which breaks in the Arrhenius plot of glucoside transport occur for similarly supplemented membranes (19). Moreover, the shape of the TEMPO solubility curve is similar for both the intact membranes and the extracted lipids.

From an analysis of the shapes of the TEMPO solubility curves on the model membrane systems, we can conclude that the abrupt changes in slope in both the TEMPO parameter curves and Arrhenius plots for the E. coli membranes can arise from three

possible sources. The high-temperature change in slope is due to the onset of phase separation, i.e., the temperature at which the transition of F phase to F + S phases begins. The low-temperature transition arises from the completion of phase separation, i.e., F + S phases going to S phase. Any other abrupt changes in slope can reflect discontinuities in the slopes of the fluidus and solidus curves (or surfaces, for a multicomponent system). The TEMPO solubility parameter depends quite strongly on the mole fraction of lipids in the F phase which in turn is quite sensitive to the shape of the phase diagram. Therefore, any sudden change in the relative shapes of the fluidus and solidus curves could produce an abrupt change in the TEMPO solubility parameter.

The elaidic acid membranes contain primarily two types of lipids: a diunsaturated phospholipid and a monounstaturated phospholipid in the ratio of about 7 to 3 (19). In this case, the two abrupt changes in slope represent the onset and completion of phase separation and the phase diagram would probably be similar to those obtained for binary mixtures of lipids which form a complete range of solid solutions, as in Fig. 3. In principle, it is possible to calculate the shape of the fluidus and solidus curves from the shape of the TEMPO solubility curve. This type of a calculation would allow us to determine the phase diagram of an intact bacterial membrane.

Linden et al. (19) observed an enhanced glucoside transport rate in the elaidic acid supplemented membranes at a temperature near the onset of phase separation. Wu and McConnell (24) also observe an enhanced valinomycin-mediated K^+ conductivity through DPPC membranes at the transition temperature of DPPC. These effects might be the result of enhanced transport at the boundaries between the F and S phases (25). In this case, the maximum effect should be observed in the middle of the "transition" where the interface between these two areas is a maximum. On the other hand, the enhanced transport could be the result of fluctuations in the surface density of the lipids in the membrane. The fluctuations would be large when both F and S phase are present since the lateral compressibility would be quite high under these conditions. This effect is likely to be a maximum when the rate of change of the lipids from the F to the S phase with temperature is a maximum. Under these conditions, the slope of the TEMPO solubility parameter–temperature curve would also be a maximum. Further studies of the relation between phase separations and transport are in progress.

ACKNOWLEDGMENTS

This research has been sponsored by the National Science Foundation under Grant GB-33501X. It has benefited from facilities made available to Stanford University by the Advanced Research Projects Agency through the Center for Materials Research. E. J. Shimshick was supported by a National Science Foundation Graduate Fellowship (1970–1973). We are indebted to Professor D. Branton for the use of the freeze-fracture apparatus used to obtain the photograph in Fig. 2.

REFERENCES

1. Frye, L. D., and Edidin, M., J. Cell. Sci. 7:313, (1970).
2. Edidin, M., "Membrane Research," C. F. Fox (Ed.), Academic Press, New York, p. 15 (1972).
3. Devaux, P., and McConnell, H. M., J. Amer. Chem. Soc. 94:4475 (1972).

4. Träuble, and Sackmann, E., J. Amer. Chem. Soc. 94:4499 (1972).
5. Scandella, C. J., Devaux, P., and McConnell, H. M., Proc. Nat. Acad. Sci. 69:2056 (1972).
6. Devaux, P., and McConnell, H. M., Ann. N.Y. Acad. Sci. (in press).
7. Devaux, P., Scandella, C. J., and McConnell, H. M., J. Mag. Res. 9:474 (1973).
8. Brown, P. K., Nature New Biology 236:35 (1972).
9. Cone, R. A., Nature New Biology 236:39 (1972).
10. Cone, R. A., private communication.
11. Chapman, D., Williams, R. M., and Ladbrooke, B. D., Chem. Phys. Lipids 1:445 (1967).
12. Luzzati, V., Tardieu, A., Gulik, T., Mateu, L., Ranck, J. L., Schechter, E., Chabre, M., and Caron, F., FEBS Abstracts, 8th Meeting, Amsterdam, August 20–25, (1972).
13. Hubbell, W. L., and McConnell, H. M., J. Amer. Chem. Soc. 93:314 (1971).
14. Hinz, H. J., and Sturtevant, J. M., J. Biol. Chem. 247:6071 (1971).
15. Barrat, M. D., Green, D. K., and Chapman, D., Chem. Phys. Lipids 3:140 (1969).
16. Overath, P., Schairer, H. U., and Stoffel, W., Proc. Nat. Acad. Sci. 67:606, (1970).
17. Esfahani, M., Limbrick, A. R., Knutton, S., Oka, T., and Wakil, S., Proc. Nat. Acad. Sci. 68:3180 (1970).
18. Fox, C. F., and Tsukagoshi, N., in "Membrane Research," C. F. Fox, (Ed.). Academic Press, New York, p. 45 (1972).
19. Linden, C., Wright, K. L., McConnell, H. M., and Fox, C. F., Proc. Nat. Acad. Sci. (in press).
20. Verkleij, A. J., Ververgaert, P. H. J., van Deenen, L. L. M., and Elbers, P. F., Biochim. Biophys. Acta 288:326 (1972).
21. Shimshick, E. J., and McConnell, H. M., Biochem. (in press).
22. Shimshick, E. J. and McConnell, H. M., Biochem. Biophys. Res. Comm. (in press).
23. Hubbell, W. L., and McConnell, H. M., Proc. Nat. Acad. Sci, 61:12 (1968).
24. Wu, S., and McConnell, H. M., (to be published).
25. Papahadjopoulos, D., Jacobson, K., Nin, S., Isac, T., Biochim. Biophys. Acta (in press).